MAJOR ARTICLE

The Extracellular Matrix Regulates Granuloma Necrosis in Tuberculosis

Basim Al Shammari,[1] Takayuki Shiomi,[9] Liku Tezera,[7] Magdalena K. Bielecka,[7] Victoria Workman,[4,5,6] Tarangini Sathyamoorthy,[1] Francesco Mauri,[2] Suwan N. Jayasinghe,[4,5,6] Brian D. Robertson,[3] Jeanine D'Armiento,[9,a] Jon S. Friedland,[1,a] and Paul T. Elkington[1,7,8]

[1]Infectious Diseases and Immunity Section, Division of Infectious Diseases, [2]Histopathology Department, Centre for Pathology, Division of Experimental Medicine, [3]MRC Centre for Molecular Bacteriology and Infection, Department of Medicine, Imperial College London, [4]BioPhysics Group, Department of Mechanical Engineering, [5]Institute of Biomedical Engineering, [6]Centre for Stem Cells and Regenerative Medicine, University College London; [7]NIHR Respiratory Biomedical Research Unit, Clinical and Experimental Sciences Academic Unit, Faculty of Medicine, and [8]Institute for Life Sciences, University of Southampton, United Kingdom; and [9]Department of Medicine, Columbia University, New York, New York

A central tenet of tuberculosis pathogenesis is that caseous necrosis leads to extracellular matrix destruction and bacterial transmission. We reconsider the underlying mechanism of tuberculosis pathology and demonstrate that collagen destruction may be a critical initial event, causing caseous necrosis as opposed to resulting from it. In human tuberculosis granulomas, regions of extracellular matrix destruction map to areas of caseous necrosis. In mice, transgenic expression of human matrix metalloproteinase 1 causes caseous necrosis, the pathological hallmark of human tuberculosis. Collagen destruction is the principal pathological difference between humanised mice and wild-type mice with tuberculosis, whereas the release of proinflammatory cytokines does not differ, demonstrating that collagen breakdown may lead to cell death and caseation. To investigate this hypothesis, we developed a 3-dimensional cell culture model of tuberculosis granuloma formation, using bioelectrospray technology. Collagen improved survival of *Mycobacterium tuberculosis*–infected cells analyzed on the basis of a lactate dehydrogenase release assay, propidium iodide staining, and measurement of the total number of viable cells. Taken together, these findings suggest that collagen destruction is an initial event in tuberculosis immunopathology, leading to caseous necrosis and compromising the immune response, revealing a previously unappreciated role for the extracellular matrix in regulating the host-pathogen interaction.

Keywords. tuberculosis; extracellular matrix; matrix metalloprotease; immunopathology.

The intensive biomedical research effort to develop new vaccination approaches and shorter treatment regimens for tuberculosis have not yet resulted in significant changes to disease management [1–3], suggesting that paradigms of pathogenesis may be incomplete. The pathophysiological hallmark of tuberculosis is caseous necrosis, which is thought to result from *Mycobacterium tuberculosis*–mediated macrophage cell death [4–6]. An excessive proinflammatory immune response may exacerbate tissue destruction [7], and this concept of pathology informs novel vaccine and immunomodulatory strategies [8, 9].

In this model of tuberculosis pathology, caseous necrosis is proposed to cause tissue destruction, leading to lung cavitation and transmission of infection [10, 11]. This long-established paradigm primarily derives from classical experiments in the rabbit model of *Mycobacterium bovis* infection, in which large tubercules develop and then rupture into the airways [12]. However, dissection of the precise sequence of events is limited by the lack of suitable animal models, since caseous necrosis is generally not observed in immunocompetent mice [13]. Caseous necrosis is observed in tuberculosis granulomas of humanized mice engrafted with fetal human liver and thymus tissue [14], while large regions of

Received 4 December 2014; accepted 29 January 2015; electronically published 12 February 2015.

Presented in part: Keystone Symposia: Novel Therapeutic Approaches to Tuberculosis, Keystone, Colorado, 30 March–4 April 2014.

[a]J. D. and J. S. F. contributed equally to this report.

Correspondence: Paul T. Elkington, MD, PhD, Clinical and Experimental Sciences, University of Southampton, Southampton SO16 1YD, UK (p.elkington@soton.ac.uk).

The Journal of Infectious Diseases® 2015;212:463–73

DOI: 10.1093/infdis/jiv076

necrosis may develop in mice that control *M. tuberculosis* proliferation poorly and develop a very high mycobacterial load [15]. However, mycobacteria are very infrequent in human granulomas [16], and therefore pathology in human disease is initially driven by a low mycobacterial load.

We have previously demonstrated that matrix metalloproteinase 1 (MMP-1)–expressing mice develop collagen destruction within granulomas when infected with *M. tuberculosis* H37Rv, the standard laboratory strain, and that this collagen destruction occurred in the absence of caseous necrosis [17]. However, the relationship between extracellular matrix destruction and the cell death that forms caseous necrosis has not been systematically examined, nor has the influence of extracellular matrix destruction on the interaction between host immune cells and *M. tuberculosis*. We reconsider the sequence of events driving immunopathology in tuberculosis by studying human lung biopsy specimens, mice expressing human MMPs, and 3-dimensional cell culture systems and conclude that collagen destruction is an early event that increases host cell death.

METHODS

Ethics Statement

The project was approved by the Hammersmith and Queen Charlotte's and Chelsea Research Ethics Committee, London (reference 07/H0707/120). Lung biopsy specimens were collected as part of routine clinical care and processed for standard diagnostic testing. The residual tissue blocks not required for diagnostic purposes were analyzed in this study and were released from the Hammersmith Hospitals National Health Service Trust Human Biomaterials Resource centre. The ethics committee approved the analysis of this tissue without receipt of individual informed consent, since it was surplus archived tissue taken as part of routine care. All animal experiments were approved by the Home Office of the United Kingdom, which is responsible for approving laboratory animal care and experiments in the United Kingdom, under project license PPL 70–7160. All experiments were performed in accordance with the United Kingdom Animal (Scientific Procedures) Act 1986 in the containment level 3 animal facility at Imperial College London. For analysis of blood specimens from healthy donors, this work was approved by the National Research Ethics Service committee South Central–Southampton A (reference 13 SC 0043), and all donors gave written informed consent.

Extracellular Matrix Staining in Human Lung Biopsy Specimens

Lung biopsy specimens obtained from patients under investigation for probable lung cancer who had pulmonary tuberculosis diagnosed as a result of the biopsy specimen appearances were studied. All patients had caseous necrosis, the pathognomonic appearance of tuberculosis, and responded well to standard antibiotic treatment. Staining with Masson's trichrome, Picrosirius red, and Elastin van Gieson was performed according to standard protocols.

Mouse *M. tuberculosis* Infection Protocol

All mice were bred on the C57BL6 background, which is relatively resistant to infection with *M. tuberculosis*. Mice expressing human MMP-1 and MMP-9 under control of the scavenger receptor A promoter/enhancer and wild-type littermates were infected intranasally with 5000 colony-forming units (CFU) of *M. tuberculosis* that had recently been isolated from a patient with pulmonary tuberculosis [18]. Preliminary studies demonstrated that this protocol reliably produced a pulmonary deposition of approximately 500 CFU and caused formation of giant cells, a characteristic feature of human disease not caused by *M. tuberculosis* H37Rv in C57BL6 mice. For each experiment, there were ≥5 mice per group, with 3 separate experiments performed. Mice were checked regularly for signs of distress and weighed fortnightly. Mice were euthanized by receipt of an overdose of anesthetic at 22 weeks and dissected as previously described [17]. For protein analysis and colony counting, 1 lobe of the lung was homogenized in 1 mL of phosphate-buffered saline (PBS). Colony counting was performed by plating on Middlebrook 7H11 agar (BD Biosciences, Oxford, United Kindom). Lung homogenate and bronchoalveolar lavage fluid were sterilized through a 0.2 μm filter (Millipore) [19].

Luminex Analysis

MMP and cytokine concentrations were analyzed on a Bioplex 200 platform (Bio-Rad, Hemel Hempstead, United Kingdom) according to the manufacturer's protocol. MMP concentrations were analyzed by MMP fluorokine multianalyte profiling (R&D Systems, Abingdon, United Kingdom), and cytokine concentrations were measured using the cytokine mouse panel (Invitrogen, United Kingdom).

2-Dimensional In Vitro Granuloma Model

We adapted the model described by F. Altare's group [20]. Peripheral blood mononuclear cells (PBMCs) were isolated from single-donor buffy coats from the National Blood Transfusion Service (Colindale, United Kingdom) or from healthy volunteers. Leukocytes were isolated by density gradient centrifugation over Ficoll-Paque (Amersham Biosciences, United Kingdom). Total PBMCs were plated on 24-well plates at 1×10^6 cells/well in 10% AB serum in Roswell Park Memorial Institute (RPMI) 1640 medium supplemented with 2 mM glutamine and 10 μg/mL ampicillin. PBMCs were infected with *M. tuberculosis* at a multiplicity of infection (MOI) of 0.001.

DQ Collagen Degradation Assay

PBMCs were resuspended in collagen mix solution composed of 8 parts sterile collagen type I (Advanced BioMatrix, San Diego, California) with DQ collagen (Invitrogen, Paisley, United Kingdom; ratio, 1:7) and 1 part sterile 10× RPMI 1640

medium, NaOH in HEPES, and AB serum. pH was corrected to 7.0, using 7.5% $NaHCO_3$. A total of 1×10^6 PBMCs were seeded in 4-well coverglass-bottomed chamber slides (PAA laboratories), and *M. tuberculosis* was added at a MOI of 0.001 to infection wells. Slides were incubated and observed under a confocal microscope (Leica).

Green Fluorescent Collagen Degradation Assay

Four-well glass-bottomed chamber slides (PAA laboratories) were coated with 0.005% poly-L-lysine (Sigma, Poole, United Kingdom) and washed sequentially with PBS, 0.5% glutaraldehyde (BDH), and PBS. Wells were coated with collagen-FITC solution (Sigma, 1 mg/mL) in 0.1 M acetic acid solution and then washed with PBS, sodium borohydride solution (Sigma), and sterile Hank's balanced salt solution (HBSS). Wells were seeded with PBMCs, infected with *M. tuberculosis*, and observed under a confocal microscope (Leica Microsystems).

Lactate Dehydrogenase (LDH) Assay

Cell culture supernatants were harvested, underwent sterile filtration (Millipore, United Kingdom), and analyzed in accordance with the manufacturers' instructions (Roche, Burgess Hill, United Kingdom).

Agar 3-Dimensional Cell Culture Model

Soft agar (1.5%, Sigma) was heated in a microwave for 2 minutes and warmed to 50°C. A final agar concentration of 0.7% was prepared with 10× RPMI 1640 medium, AB serum (10%), 1 M HEPES, 7.5% $NaHCO_3$, and distilled water. PBMCs were incorporated in agar with or without collagen, and the gel was allowed to set at 37°C. RPMI 1640 medium with 10% AB serum was added to the wells, and samples were obtained at predetermined time points.

Cell Encapsulation Using an Electrostatic Bead Generator

PBMCs were isolated and embedded into alginate microspheres, using an electrostatic bead generator (Nisco, Zurich, Switzerland) as described elsewhere [21]. Briefly, PBMCs were mixed with sterile alginate mix (3% [Sigma, United Kingdom] or Pronova UP MVG alginate [NovaMatrix, Norway]) in HBSS without Ca/Mg, 1 M HEPES, and 7.5% $NaHCO_3$ to a final concentration of 5×10^6 cells/mL. Purified human collagen solution (VitroCol, Advanced BioMatrix) was added at 1 mg/mL for alginate-collagen microspheres. *Mycobacterium tuberculosis*–stimulated microspheres were generated by adding either UV-killed *M. tuberculosis* H37Rv or bioluminescent *M. tuberculosis* H37Rv expressing the Lux operon at a MOI 0.1 to the alginate solution prior to microsphere generation.

Alginate suspension containing cells, with or without *M. tuberculosis* and with or without collagen, was injected via a Harvard syringe driver into the bead generator at 10 mL/hour, using a bioelectrospray needle with a 0.7-mm external diameter. Microspheres were formed by ionotropic gelling in 100 mM calcium chloride. Microspheres were then washed twice with HBSS, placed in RPMI 1640 medium supplemented with 10% AB serum, and incubated at 37°C. Supernatant surrounding the microspheres was harvested at defined time points.

Immunofluorescence and Confocal Imaging

Microspheres were fixed in 4% paraformaldehyde, washed in PBS, and stained with DAPI (4′,6-diamidino-2-phenylindole) or calcein. Confocal images were acquired on a Leica SPE microscope with an APO 40×1.15 NA oil immersion lens.

Flow Cytometry

Cells were extracted from microspheres by dissolving in 15 mM ethylenediaminetetraacetic acid in PBS for 10 minute at 37°C. Cells were suspended in PBS containing 50 μg/mL propidium iodide, and fluorescence was analyzed by flow cytometry (BD Accuri C6 flow cytometer). Three replicates were taken for each experiment, and 10 000 cells were acquired for each sample. Experiments were repeated at least 3 times.

Cell Viability Assay

Microspheres containing PBMCs infected with UV-killed *M. tuberculosis* at MOI of 0.1 were generated from alginate, alginate-collagen (Advanced BioMatrix), or alginate-gelatin (Sigma). Microspheres were incubated in 96-well plates for 4 days at 37°C. Cell viability was analyzed using the CellTiter-Glo 3D Cell Viability Assay (Promega) according to the manufacturer's instructions. Luminescence was analyzed by the GloMax Discover system (Promega).

Statistical Analysis

Paired groups were compared by the Student *t* test, while multiple groups were analyzed by 1-way analysis of variance. Differences were considered significant at $P < .05$.

RESULTS

Caseous Necrosis Maps to Regions of Collagen Destruction in Human Pulmonary Granulomas

First, we investigated extracellular matrix integrity and caseous necrosis in lung granulomas from patients with pulmonary tuberculosis (Figure 1 and Supplementary Figure 1). Sirius red staining demonstrated that collagen was intact where cells had a normal morphology, whereas in areas of caseous necrosis no collagen was visualized (Figure 1*A* and 1*B*). Elastin–van Giesen staining demonstrated that no elastin was present in these regions (Figure 1*C* and 1*D*). Similarly, Masson's trichrome staining showed that extracellular matrix was absent in areas of caseous necrosis (Supplementary Figure 1). Therefore, in patients with pulmonary tuberculosis, caseous necrosis and extracellular matrix destruction are observed concurrently, but whether cell death or extracellular matrix destruction is the initial pathological event cannot be determined.

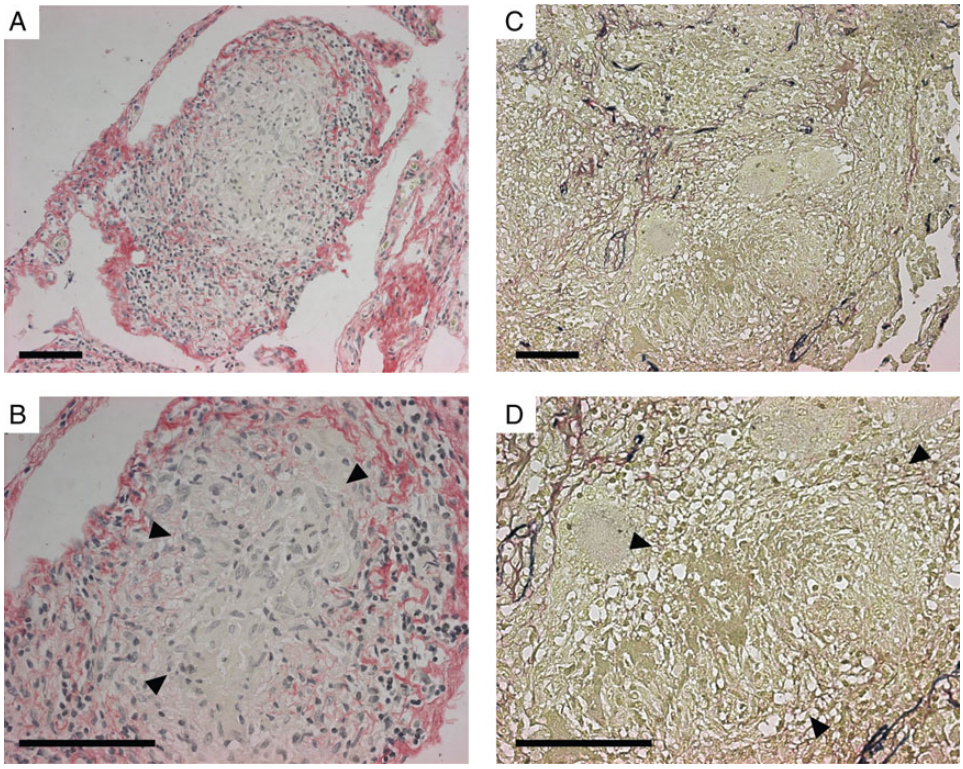

Figure 1. Lung extracellular matrix destruction and caseous necrosis colocalize in human pulmonary granulomas. Lung biopsy specimens from patients who were under investigation for lung carcinoma but received a final diagnosis of tuberculosis on the basis of histological findings were stained by Picrosirius red (*A* and *B*; collagen fibrils stain red), and elastin–van Gieson (*C* and *D*; elastin fibrils stain blue). Arrowheads designate areas of caseous necrosis. Collagen and elastin fibrils are absent in all regions of caseous necrosis. Images are representative of lung biopsy specimens from 5 patients with tuberculosis. Scale bars, 100 μm.

Expression of Human MMP-1 in Mice Causes Caseous Necrosis in Tuberculosis Granulomas

To address the relationship between extracellular matrix destruction and cell death, we infected mice expressing human MMP-1 under control of the scavenger receptor A promoter/enhancer [22] with a clinical strain of *M. tuberculosis* recently isolated from a patient with pulmonary tuberculosis. All mice were bred on the C57BL6 background, which is relatively resistant to mycobacterial infection, and were infected with 5000 CFU intranasally, resulting in a pulmonary infectious dose of 500 CFU. In preliminary studies, we demonstrated that this strain caused pathological features typical of human tuberculosis that were not observed after infection with *M. tuberculosis* H37Rv in C57BL6 mice. C57BL6 mice expressing human MMP-9 regulated by the same promoter acted as controls for the transgenic expression of a human MMP. In all infected mice, multinucleate giant cells were observed within granulomas, implying that multinucleate giant cells result from infection with *M. tuberculosis* that has not undergone prolonged laboratory subculture (Figure 2*A*–*C*). No difference in colony counts or weight loss occurred between strains, demonstrating that human MMP expression did not modulate control of *M. tuberculosis* growth (Figure 2*D* and 2*E*). Total lung inflammation was similar between mice (Supplementary Figure 2), and *M. tuberculosis* was visualized on Ziehl-Neelsen staining of granulomas in each mouse strain (Supplementary Figure 3). *Mycobacterium tuberculosis* infection upregulated human MMP-1 and MMP-9 expression in the respective transgenic mice (Figure 2*F* and 2*G*). In the MMP-1–expressing mice, areas of tissue destruction were observed within the center of granulomas (Figure 2*K*–*M*) that did not occur in wild-type or MMP-9–expressing mice (Figure 2*H*–*J* and 2*N*–*P*). These regions contained amorphous debris with no cellular structure, typical of caseous necrosis observed in human tuberculosis. Therefore, MMP-1–expressing mice demonstrate pathology characteristic of human tuberculosis, which is not seen in other immunocompetent mice of diverse genetic backgrounds [13] unless they are either humanized or have a very high mycobacterial load [14, 15].

To determine whether caseous necrosis resulted from an imbalance in T-helper type 1 (Th1)/Th2 immunity, as was postulated elsewhere [6], we profiled cytokines and chemokines in lung homogenate and bronchial lavage fluid by Luminex array. *Mycobacterium tuberculosis* infection upregulated tumor necrosis factor α, interleukin 1β, interleukin 12, interferon γ, monocyte

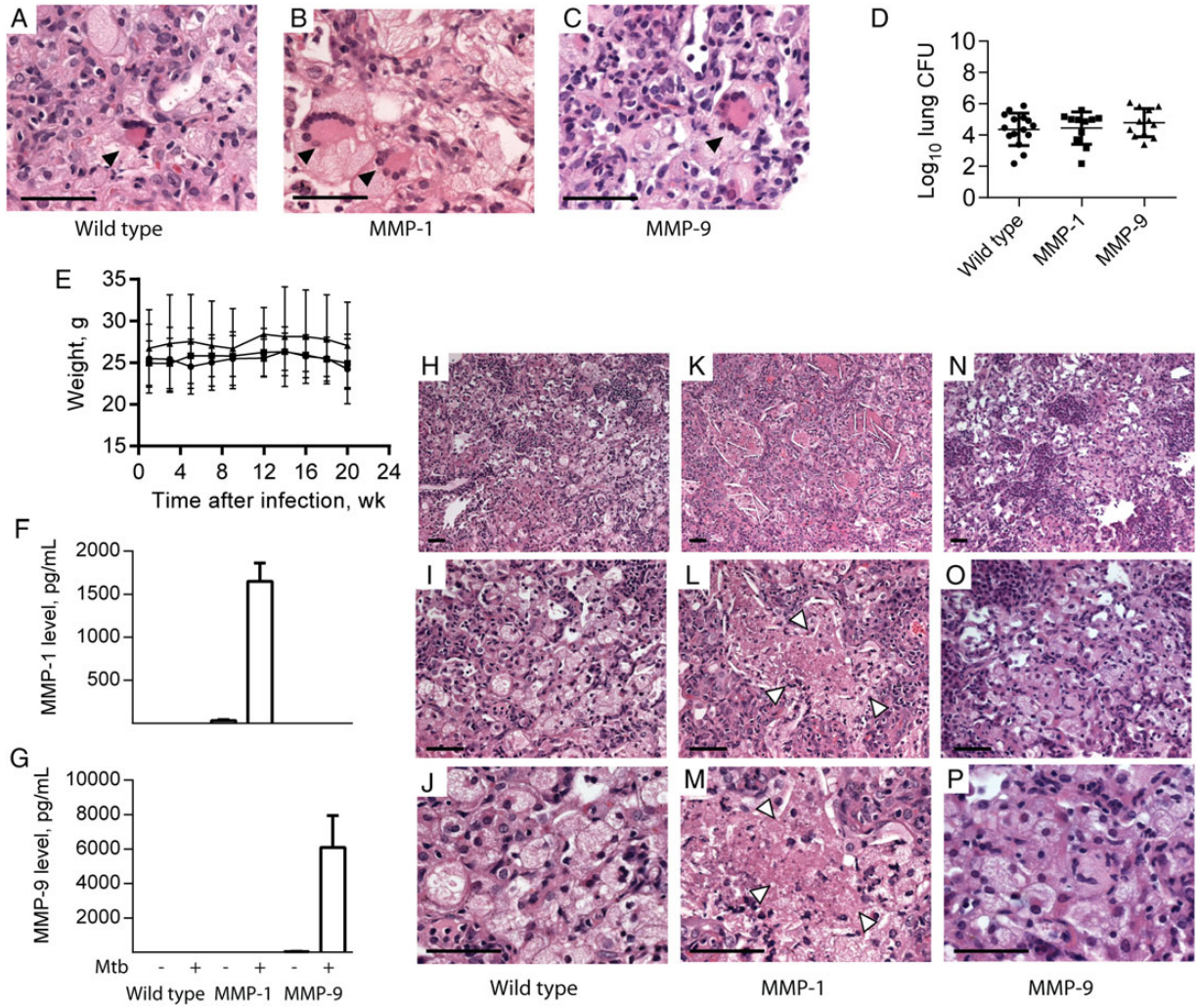

Figure 2. Mice expressing human matrix metalloproteinase 1 (MMP-1) develop regions of caseous necrosis in tuberculosis granulomas. Mice expressing human MMP-1 or MMP-9 and their wild-type littermates were infected with an Indo-Oceanic strain of *Mycobacterium tuberculosis* recently isolated from a patient with pulmonary tuberculosis. Mice were euthanized 22 weeks after infection. *A–C*, All mice strains developed multinucleate giant cells in regions of macrophage infiltration (arrowheads). *D*, No difference in mycobacterial growth was observed between mice strains. Horizontal lines denote mean values, with bars denoting standard deviations (SDs). *E*, Mouse weights did not differ between strains during the course of infection. Circles denote wild-type mice, squares denote MMP-1–expressing mice, and triangles denote MMP-9–expressing mice, with mean values and SDs denoted by lines and whiskers, respectively. *F* and *G*, Infection upregulated human MMP-1 and MMP-9 in lung homogenates of the respective transgenic mice. Mean values plus standard errors of the mean are shown. *H–P*, In the MMP-1–expressing mice, regions of tissue destruction developed (arrowheads), with amorphous central material typical of human caseous necrosis (*K*, *L*, and *M*), which was not observed in similar granulomas in wild-type mice (*H*, *I*, and *J*) or MMP-9–expressing mice (*N*, *O*, and *P*). The experiment was performed 3 times, with a minimum of 5 mice per group. Scale bars, 25 μm. Abbreviation: CFU, colony-forming units.

chemotactic protein 1, and IFN-γ–inducible protein 10 in all mouse strains, but no difference in cytokine profile was demonstrated (Figure 3*A–F*). This suggested that the observed caseous necrosis did not result from MMP-1 expression having an immunomodulatory effect. Interleukin 6 concentrations were below the level of sensitivity of the assay. The only difference between the MMP-1–expressing mice and their wild-type littermates is the expression of a collagenase, leading us to examine extracellular matrix integrity within granulomas. In all areas of caseous necrosis, collagen was destroyed (Figure 3*H*), whereas in wild-type mice and MMP-9–expressing mice, the extracellular matrix was intact, and cells appeared viable within tuberculosis granulomas (Figure 3*G* and 3*I* and Supplementary Figure 4).

Collagen Improves Survival of *M. tuberculosis*–Infected Human Cells

The development of caseous necrosis in MMP-1–expressing mice suggested that the initial event in tuberculosis immunopathology is collagen destruction, which leads to cell death, as opposed to the current paradigm, in which collagen destruction is

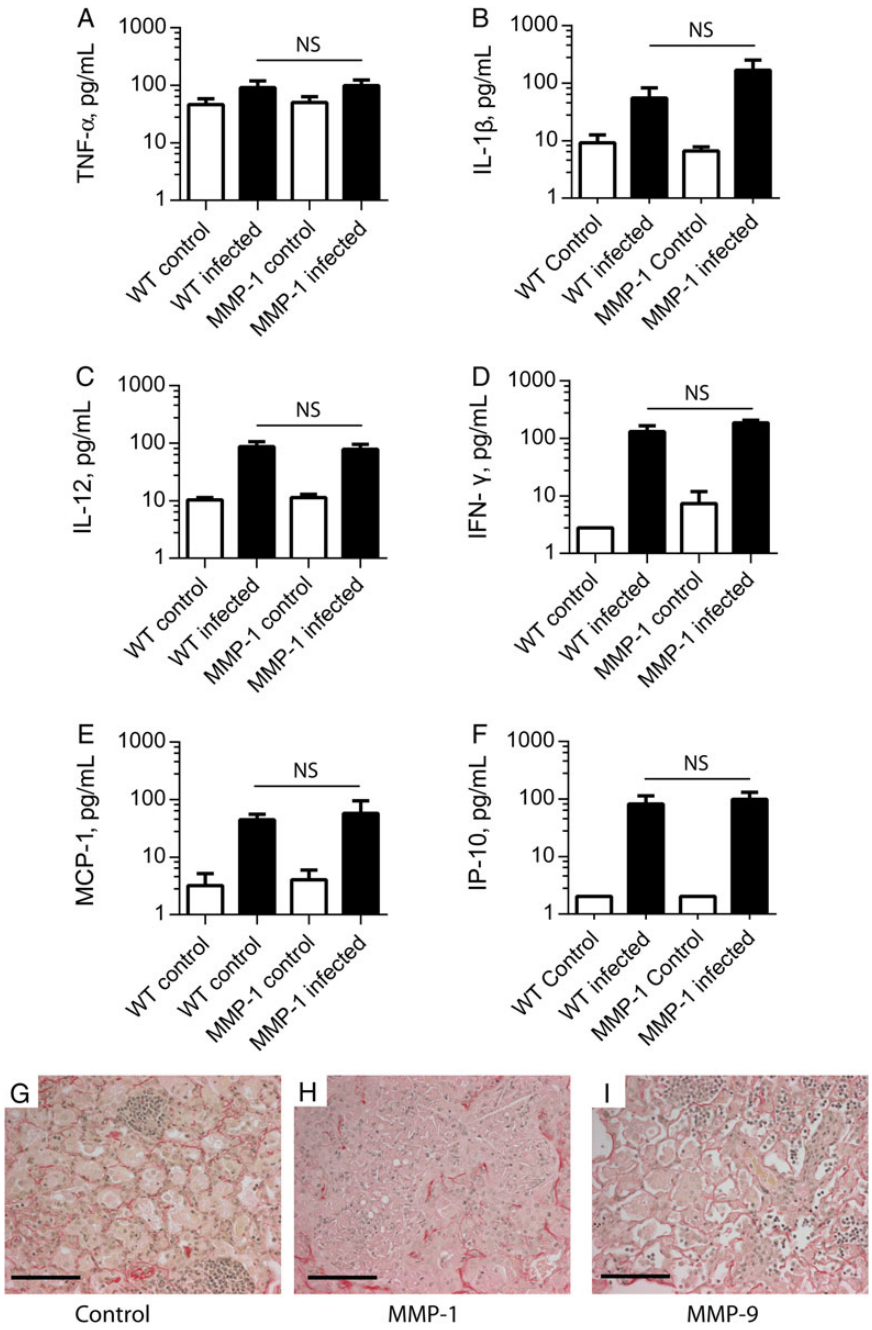

Figure 3. Cytokine secretion does not differ between matrix metalloproteinase 1 (MMP-1)–expressing mice and wild-type (WT) mice, but collagen is absent in regions of caseous necrosis. *A–F*, Concentrations of tumor necrosis factor α (TNF-α), interleukin 1β (IL-1β), interleukin 12 (IL-12), interferon γ (IFN-γ), monocyte chemotactic protein 1 (MCP-1), and IFN-γ–inducible protein 10 (IP-10) were measured in mouse lung homogenates at 22 weeks after infection by Luminex array. *Mycobacterium tuberculosis* infection upregulated each of these proinflammatory mediators in all infected mice, but there were no significant differences related to the genotype of the mice. Open bars denote uninfected mice, and filled bars denote *M. tuberculosis*–infected mice. Mean values ± standard errors of the mean are shown. *G–I*, Total collagen was analyzed by Picrosirius red staining. In wild-type mice (*G*) and matrix metalloproteinase 9 (MMP-9)–expressing mice (*I*), alveolar wall collagen remained intact in regions of macrophage infiltration. However, in MMP-1–expressing mice, collagen was destroyed and colocalized with regions of caseous necrosis (*H*). Data are representative of 5 mice per group infected in 3 independent experiments. Scale bars, 50 μm. Abbreviation: NS, not significant.

believed to occur secondary to cell death. To test this hypothesis, we first analyzed a 2-dimensional cell culture in vitro granuloma model incorporating PBMCs and live *M. tuberculosis* [23]. Human granulomas contain very few mycobacteria relative to inflammatory cells [16], so a low MOI was used to reflect clinical disease. Granulomas formed over time (Figure 4*A*).

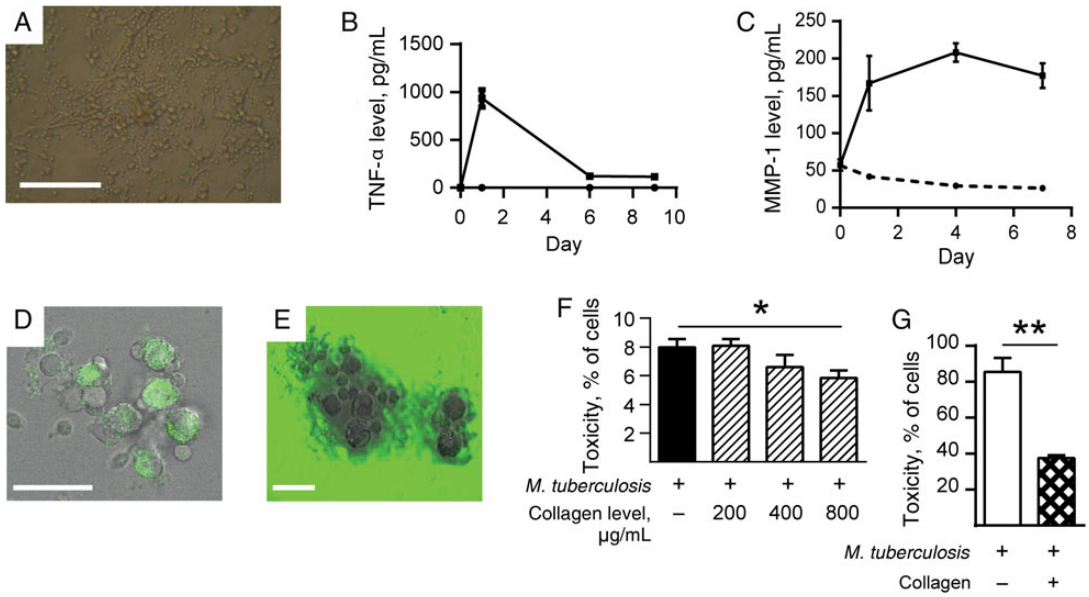

Figure 4. Collagen improves survival of *Mycobacterium tuberculosis*–infected cells in a 2-dimensional primary human cell culture system. Primary human peripheral blood mononuclear cells were infected with *M. tuberculosis* H37Rv in 24-well tissue culture plates and observed for 15 days. *A*, Cellular aggregates developed in *M. tuberculosis*–infected wells by day 4. *B* and *C*, *M. tuberculosis* infection increases secretion of tumor necrosis factor α (TNF-α) and matrix metalloproteinase 1 (MMP-1) in cell culture supernatants analyzed by Luminex array. *D*, Aggregates cause pericellular collagen destruction, analyzed by coculture with DQ-labeled collagen, which gains fluorescence when cleaved (*E*), or with fluorescent collagen, which loses fluorescence when degraded. *F*, Addition of collagen to *M. tuberculosis*–infected cells reduces cell death, as analyzed by the lactate dehydrogenase release assay. *G*, In a 3-dimensional model in which cells and *M. tuberculosis* are incorporated into an agar matrix with or without addition of collagen, incorporation of collagen with cells improves cellular survival after *M. tuberculosis* infection. Each experiment was performed a minimum of 2 times. Charts demonstrate the mean values + standard errors of the mean of a representative experiment performed in triplicate. Scale bars, 100 μm (*A*) and 25 μm (*D* and *E*). $^{*}P < .05$, $^{**}P < .01$.

Mycobacterium tuberculosis infection increased MMP and cytokine expression (Figure 4*B* and 4*C* and Supplementary Figure 5). To quantitate the functional effect of MMP activity on extracellular matrix turnover, cells were plated on slides coated with DQ-labeled collagen, which becomes fluorescent when degraded, or fluorescent collagen, which loses fluorescence when cleaved. The increased MMP activity caused collagen degradation by both assays (Figure 4*D* and 4*E*). Addition of human collagen to the cell culture medium improved cellular survival after *M. tuberculosis* infection (Figure 4*F*). However, cell–extracellular matrix interactions occur in a 3-dimensional framework, and therefore we studied 3-dimensional granuloma models impregnated with diverse matrices. In an agar 3-dimensional model, incorporation of collagen improved cellular survival after *M. tuberculosis* stimulation, compared with cells in an agar matrix without collagen (Figure 4*G*).

To further investigate this observation, we developed a 3-dimensional cell culture model of tuberculosis granuloma formation, since cell–extracellular matrix interactions occur in 3 dimensions. This model permitted investigation of the hypothesis that extracellular matrix composition regulates the host-pathogen interaction without the need for extensive animal modeling. We used a bioelectrospray system to generate microspheres incorporating alginate, which cross-links in a gelling bath containing calcium chloride and permits regulation of the cellular and extracellular matrix fibrillar composition within the microspheres (Figure 5*A* and 5*B*) [21]. Monocytes within the microspheres phagocytosed *M. tuberculosis* (Figure 5*C*), and progressive cellular aggregation occurred in infected microspheres over time (Figure 5*D*). *Mycobacterium tuberculosis* infection led to a progressive increase in chemokine and MMP accumulation in the cell culture medium, demonstrating that inflammatory mediators that increase during human tuberculosis were induced in this model (Figure 5*E* and 5*F*). To determine whether the extracellular matrix regulated cellular survival, human type I collagen was incorporated into microspheres. Cells in collagen-impregnated microspheres survived better when infected with *M. tuberculosis*, according to results of an LDH release assay (Figure 5*G* and 5*H*) and flow cytometry (Figure 5*I*). Furthermore, total viable cell numbers in collagen-containing microspheres were higher than in alginate-only microspheres (Figure 5*J*). In contrast, incorporation of gelatin into the microspheres did not increase cellular viability (Figure 5*J*). These data confirm that cells adherent to collagen fibrils have greater survival when infected with *M. tuberculosis* than those without extracellular matrix contact.

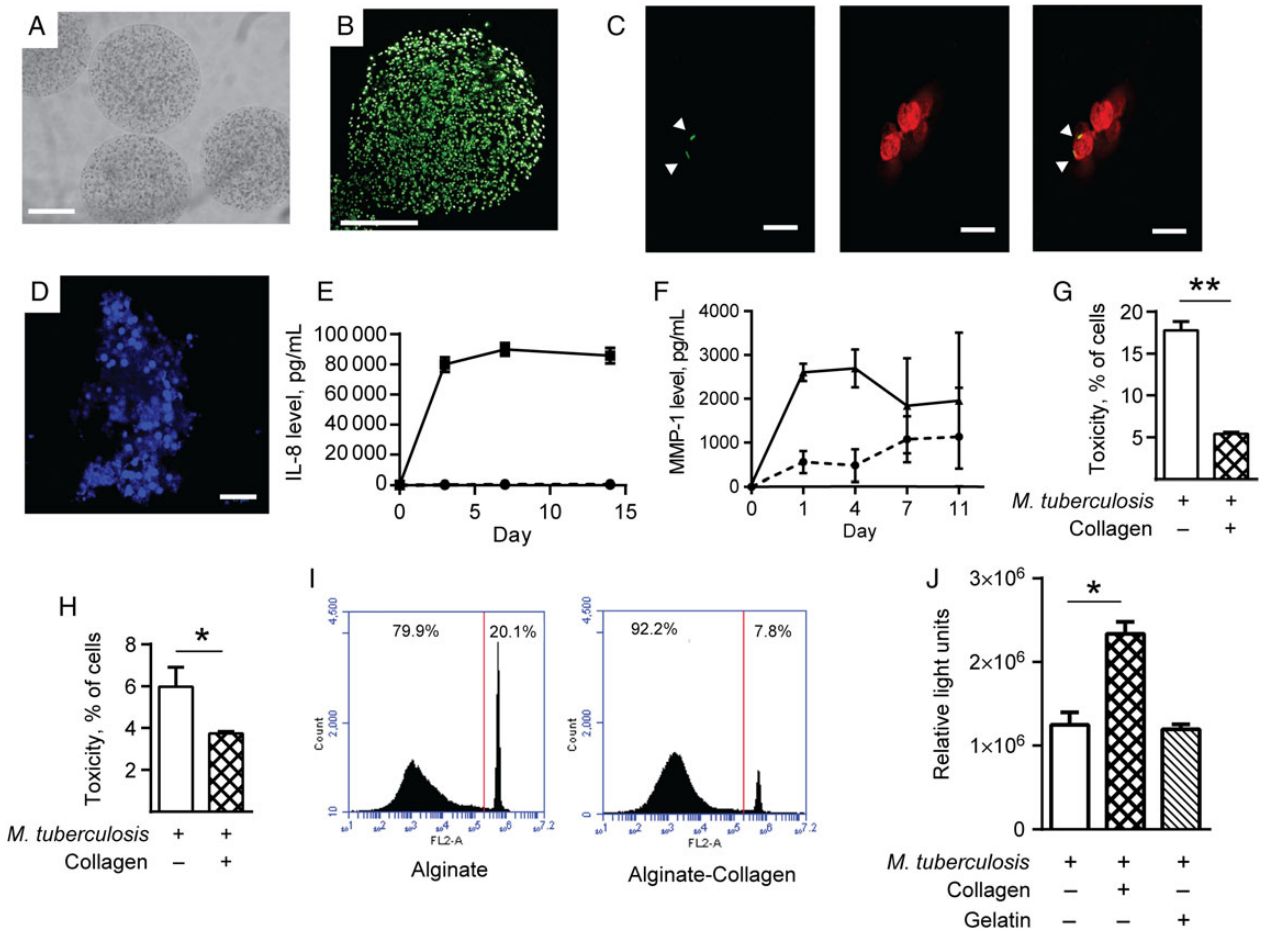

Figure 5. A 3-dimensional bioelectrospray granuloma model demonstrates collagen improves cellular survival after *Mycobacterium tuberculosis* infection. Alginate microspheres were generated by bioelectrospraying a mixture of sterile alginate and peripheral blood mononuclear cells (PBMCs), with or without the incorporation of *M. tuberculosis* H37Rv and/or collagen into a gelling bath, which cross-links alginate to form microspheres. *A*, Microspheres imaged immediately after bioelectrospraying by light microscopy. *B*, Calcein staining of cells immediately after bioelectrospraying shows even distribution of cells throughout the microsphere. *C*, Cells within microspheres phagocytose green fluorescent protein (GFP)–expressing *M. tuberculosis* after 4 days. GFP-expressing *M. tuberculosis* (green) are phagocytosed by monocytes (red) in the overlayed image (arrowheads indicate GFP-labeled *M. tuberculosis*). *D*, Large multicellular aggregates develop within *M. tuberculosis*–stimulated microspheres after 11 days, imaged after nuclear staining with DAPI. *E* and *F*, Interleukin 8 (IL-8) and matrix metalloproteinase 1 (MMP-1) progressively accumulate in medium surrounding microspheres containing PBMCs infected with *M. tuberculosis*. Broken line denotes uninfected PBMCs, and filled lines denote *M. tuberculosis*-infected PBMCs. *G*, Incorporation of collagen into microspheres improves survival of THP-1 cells after *M. tuberculosis* infection, as analyzed by analyzed by the lactate dehydrogenase release assay. *H*, Similarly, PBMCs show greater survival when infected in microspheres containing collagen. *I*, Collagen improves viability of PBMCs infected with *M. tuberculosis* within microspheres when analyzed by propidium iodide staining. *J*, Total cell numbers are increased in *M. tuberculosis*–infected collagen-containing microspheres, analyzed by ATP released from viable cells. All experiments were performed a minimum of 2 times. For charts, data represent mean values ± standard errors of the mean of experiments performed in triplicate. Scale bars, 250 μm (*A* and *B*), 10 μm (*C*), and 20 μm (*D*). $^{*}P < .05$, $^{**}P < .01$.

DISCUSSION

Taken together, our human, mouse, and cellular data implicate collagen destruction as an early event in tuberculosis pathogenesis, leading to the development of caseous necrosis and skewing the immune response in favor of the pathogen. Collagen breakdown reduces the survival of *M. tuberculosis*–infected cells. Collagen had a more pronounced effect on cell survival in 3-dimensional cell culture than in 2-dimensional cell culture, consistent with the emerging concept that analysis of cell biology in 3 dimensions may recapitulate in vivo cellular behavior more accurately than in standard tissue culture [24]. Collagen destruction preceding caseation in tuberculosis opposes the widely held disease paradigm that extracellular matrix destruction is a consequence of caseous necrosis [4, 6] and leads to a novel concept of tuberculosis immunopathology whereby extracellular matrix destruction is the initial pathological event (Figure 6). This model is consistent with studies in cancer, where the extracellular matrix is known to be a cell survival factor [25]. However, human biopsy studies only provide data from

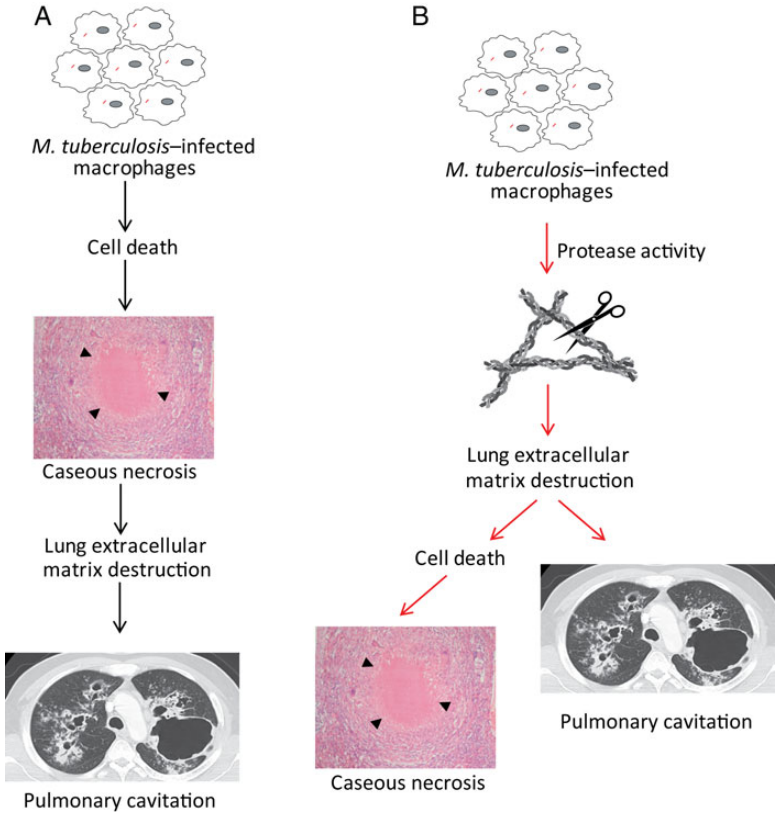

Figure 6. A novel paradigm of tuberculosis pathology. *A*, The current model of tuberculosis pathology proposes that cell death leads to caseous necrosis, which then causes lung extracellular matrix destruction, resulting in pulmonary cavitation and transmission. *B*, Our data suggest that the initial pathological event is proteolytic destruction of the lung extracellular matrix, which then leads to cell death, resulting in the accumulation of caseous necrosis and cavitation.

a single disease time point and consequently cannot determine the precise chronology of events. Ultimate proof of this concept will require MMP inhibition studies in an animal model that recapitulates the key pathological features of human tuberculosis, such as the rabbit [26], with demonstration that collagenase inhibition reduces *M. tuberculosis*–driven immunopathology.

Matrix regulation of the host immune response to tuberculosis has widespread implications, but the role of the extracellular matrix in tuberculosis tends not to be considered [4, 6, 27]. We demonstrated that collagen increased survival of cells infected with *M. tuberculosis*, whereas gelatin did not, showing that intact collagen fibrils are required. The extracellular matrix has numerous components, such as fibronectin, elastin, laminin, other collagen subtypes, proteoglycans, and hyaluronan [28], and similarly these molecules may modulate the host-pathogen interaction in tuberculosis [29]. Such cell–extracellular matrix interactions can be predicted to affect multiple key processes in the immune response to tuberculosis. For example, the extracellular matrix can modulate phagolysosomal fusion [30], proinflammatory cytokine secretion [31], autophagy [32], and immune cell activation [29]. Furthermore, cell–extracellular matrix interactions regulate cell survival [33], which is central to the host-pathogen interaction in tuberculosis [34]. In epithelial cells, integrin-dependent activation of intracellular signaling pathways via the epidermal growth factor receptor regulate cellular survival [25, 35], and in monocytes, extracellular matrix adhesion modulates gene expression profiles via integrins [36]. However, in tuberculosis, the in vitro experiments dissecting intracellular signaling pathways have almost entirely been performed in the absence of extracellular matrix.

Certain transgenic mouse models of tuberculosis may develop large regions of tissue destruction in the context of very high mycobacterial loads [15]. Lesions are marked by pronounced neutrophil infiltration, and therefore extracellular matrix destruction may be driven by MMP-8 (neutrophil collagenase), since neutrophils are the only cells that contain presynthesized MMPs. Therefore, different proteases from diverse cell types may drive pathology at different stages of tuberculosis. We focused on MMP-1, since unbiased analysis of MMPs in tuberculosis suggest that this is a dominant collagenase [26, 37, 38], but at late stages of infection neutrophil-derived MMP-8 is also likely to drive collagen destruction [39]. Similarly, stromal

cells such as epithelial cells and fibroblasts may be key sources of MMPs in inflammatory foci [40]. Our data suggest that macrophage-derived MMP-1 causes initial collagen destruction within the granuloma, leading to reduced cell survival. *Mycobacterium tuberculosis* H37Rv did not cause caseous necrosis or formation of multinucleate giant cells in infected mice, whereas these pathologies were observed after infection with a recently isolated clinical strain of *M. tuberculosis*. This implies that the prolonged laboratory culture of H37Rv since its isolation from a patient in 1905 [41] has resulted in loss of currently unidentified factors that cause giant cell formation and caseous necrosis despite being able to proliferate rapidly.

The process of caseation is likely to involve additional pathological processes that cannot be dissected our in vitro model. Diverse animal models demonstrate that tuberculosis granulomas are hypoxic [42], and in humans, vascular supply to areas of *M. tuberculosis* infection is occluded [43]. Hypoxia and inflammation have a complex interplay, and hypoxia can augment MMP release [44]. The bioelectrospray model currently incorporates PBMCs and so cannot investigate the role of neutrophils or stromal cells, which all contribute to tuberculosis pathogenesis [39, 45]. More-advanced ex vivo organ culture or in vivo experiments in an animal model in which pathology reflects disease in humans will be required to fully dissect the interplay of extracellular matrix destruction, hypoxia, and intercellular signaling.

A central role for extracellular matrix breakdown in tuberculosis pathology is supported by unbiased approaches. For example, a study comparing the macrophage gene expression profile among patients with pulmonary tuberculosis to that among individuals with latent infection identified MMP-1 as the most divergently regulated gene [46], suggesting that excessive extracellular matrix destruction is a predisposing factor in the development of tuberculosis. Similarly, MMP-1 is one of the most highly upregulated genes in infected human lung tissue [37]. A recent aptamer-based approach identified the protease-antiprotease balance and tissue remodeling as 2 key pathways that change during tuberculosis treatment, whereas cytokine pathways were not highly represented [47]. All tuberculosis treatments in the preantibiotic era, such as artificial pneumothorax, plombage, and thoracoplasty, centered on cavity collapse, and these had a cure rate of up to 70% [48], demonstrating that macroscopic stabilization of the extracellular matrix can improve host control of *M. tuberculosis* infection.

Tissue damage is emerging as a central determinant of the outcome of the host-pathogen interaction in other lung infections, such as bacterial-viral coinfection [49], supporting the hypothesis that preserving the integrity of the extracellular matrix is fundamental to an effective response to infection. Our data demonstrate that destruction of the lung extracellular matrix is likely to be an earlier event in the pathogenesis of tuberculosis than previously thought. Host-directed therapies are emerging as a novel paradigm in tuberculosis treatment [50]. Strategies to stabilize the extracellular matrix in patients with tuberculosis may not only reduce morbidity and mortality, but also may help restore an efficacious immune response to *M. tuberculosis* infection.

Supplementary Data

Supplementary materials are available at *The Journal of Infectious Diseases* online (http://jid.oxfordjournals.org). Supplementary materials consist of data provided by the author that are published to benefit the reader. The posted materials are not copyedited. The contents of all supplementary data are the sole responsibility of the authors. Questions or messages regarding errors should be addressed to the author.

Notes

Acknowledgments. We thank G. Thwaites, for providing the Indo-Oceanic strain of *M. tuberculosis*; and Siouxsie Wiles and Nuria Andreu, for providing the luminescent *M. tuberculosis*.

Financial support. This work was supported by the King Abdullah Scholarship Program (to B. A. S.), a HEFCE New Investigator award (to P. T. E.), the National Institutes of Health (grant AI102239 to P. T. E., S. N. J. and J. D.), the National Centre for the Replacement, Refinement, and Reduction of Animals in Research (NC/L001039/1 to P. T. E. and L. T.), and the National Institute for Health Research Biomedical Research Centre funding scheme at Imperial College (to J. S. F.).

Potential conflicts of interest. All authors: No potential conflicts of interest.

All authors have submitted the ICMJE Form for Disclosure of Potential Conflicts of Interest. Conflicts that the editors consider relevant to the content of the manuscript have been disclosed.

References

1. Tameris MD, Hatherill M, Landry BS, et al. Safety and efficacy of MVA85A, a new tuberculosis vaccine, in infants previously vaccinated with BCG: a randomised, placebo-controlled phase 2b trial. Lancet **2013**; 381:1021–8.
2. Johnson JL, Hadad DJ, Dietze R, et al. Shortening treatment in adults with noncavitary tuberculosis and 2-month culture conversion. Am J Respir Crit Care Med **2009**; 180:558–63.
3. Zumla A, Hafner R, Lienhardt C, Hoelscher M, Nunn A. Advancing the development of tuberculosis therapy. Nat Rev Drug Discov **2012**; 11: 171–2.
4. Cooper AM. Cell-mediated immune responses in tuberculosis. Annu Rev Immunol **2009**; 27:393–422.
5. Barry CE III, Boshoff HI, Dartois V, et al. The spectrum of latent tuberculosis: rethinking the biology and intervention strategies. Nat Rev Microbiol **2009**; 7:845–55.
6. O'Garra A, Redford PS, McNab FW, Bloom CI, Wilkinson RJ, Berry MP. The immune response in tuberculosis. Annu Rev Immunol **2013**; 31:475–527.
7. Cooper AM, Torrado E. Protection versus pathology in tuberculosis: recent insights. Curr Opin Immunol **2012**; 24:431–7.
8. Uhlin M, Andersson J, Zumla A, Maeurer M. Adjunct immunotherapies for tuberculosis. J Infect Dis **2012**; 205(suppl 2):S325–34.
9. Kaufmann SH. Future vaccination strategies against tuberculosis: thinking outside the box. Immunity **2010**; 33:567–77.
10. Dye C, Williams BG. The population dynamics and control of tuberculosis. Science **2010**; 328:856–61.
11. Russell DG, Barry CE III, Flynn JL. Tuberculosis: what we don't know can, and does, hurt us. Science **2010**; 328:852–6.
12. Dannenberg AM Jr, Sugimoto M. Liquefaction of caseous foci in tuberculosis. Am Rev Respir Dis **1976**; 113:257–9.
13. Young D. Animal models of tuberculosis. Eur J Immunol **2009**; 39: 2011–4.

14. Calderon VE, Valbuena G, Goez Y, et al. A humanized mouse model of tuberculosis. PLoS One **2013**; 8:e63331.
15. Pan H, Yan BS, Rojas M, et al. Ipr1 gene mediates innate immunity to tuberculosis. Nature **2005**; 434:767–72.
16. Park DY, Kim JY, Choi KU, et al. Comparison of polymerase chain reaction with histopathologic features for diagnosis of tuberculosis in formalin-fixed, paraffin-embedded histologic specimens. Arch Pathol Lab Med **2003**; 127:326–30.
17. Elkington P, Shiomi T, Breen R, et al. MMP-1 drives immunopathology in human tuberculosis and transgenic mice. J Clin Invest **2011**; 121:1827–33.
18. Krishnan N, Malaga W, Constant P, et al. *Mycobacterium tuberculosis* lineage influences innate immune response and virulence and is associated with distinct cell envelope lipid profiles. PLoS One **2011**; 6: e23870.
19. Elkington PT, Green JA, Friedland JS. Filter sterilization of highly infectious samples to prevent false negative analysis of matrix metalloproteinase activity. J Immunol Methods **2006**; 309:115–9.
20. Puissegur MP, Botanch C, Duteyrat JL, Delsol G, Caratero C, Altare F. An in vitro dual model of mycobacterial granulomas to investigate the molecular interactions between mycobacteria and human host cells. Cell Microbiol **2004**; 6:423–33.
21. Workman VL, Tezera LB, Elkington PT, Jayasinghe SN. Controlled generation of microspheres incorporating extracellular matrix fibrils for three-dimensional cell culture. Adv Funct Mater **2014**; 24:2648–57.
22. Lemaitre V, O'Byrne TK, Borczuk AC, Okada Y, Tall AR, D'Armiento J. ApoE knockout mice expressing human matrix metalloproteinase-1 in macrophages have less advanced atherosclerosis. J Clin Invest **2001**; 107:1227–34.
23. Puissegur MP, Lay G, Gilleron M, et al. Mycobacterial lipomannan induces granuloma macrophage fusion via a TLR2-dependent, ADAM9- and beta1 integrin-mediated pathway. J Immunol **2007**; 178:3161–9.
24. Schwartz MA, Chen CS. Cell biology. Deconstructing dimensionality. Science **2013**; 339:402–4.
25. Meredith JE Jr, Fazeli B, Schwartz MA. The extracellular matrix as a cell survival factor. Mol Biol Cell **1993**; 4:953–61.
26. Kubler A, Luna B, Larsson C, et al. *Mycobacterium tuberculosis* dysregulates MMP/TIMP balance to drive rapid cavitation and unrestrained bacterial proliferation. J Pathol **2015**; 235:431–44.
27. Elkington PT, D'Armiento JM, Friedland JS. Tuberculosis immunopathology: the neglected role of extracellular matrix destruction. Sci Transl Med **2011**; 3:71ps6.
28. Davidson JM. Biochemistry and turnover of lung interstitium. Eur Respir J **1990**; 3:1048–63.
29. Sorokin L. The impact of the extracellular matrix on inflammation. Nat Rev Immunol **2010**; 10:712–23.
30. Newman SL, Gootee L, Kidd C, Ciraolo GM, Morris R. Activation of human macrophage fungistatic activity against Histoplasma capsulatum upon adherence to type 1 collagen matrices. J Immunol **1997**; 158: 1779–86.
31. Merline R, Moreth K, Beckmann J, et al. Signaling by the matrix proteoglycan decorin controls inflammation and cancer through PDCD4 and MicroRNA-21. Sci Signal **2011**; 4:ra75.
32. Lock R, Debnath J. Extracellular matrix regulation of autophagy. Curr Opin Cell Biol **2008**; 20:583–8.
33. Buchheit CL, Rayavarapu RR, Schafer ZT. The regulation of cancer cell death and metabolism by extracellular matrix attachment. Semin Cell Dev Biol **2012**; 23:402–11.
34. Behar SM, Divangahi M, Remold HG. Evasion of innate immunity by *Mycobacterium tuberculosis*: is death an exit strategy? Nat Rev Microbiol **2010**; 8:668–74.
35. Moro L, Venturino M, Bozzo C, et al. Integrins induce activation of EGF receptor: role in MAP kinase induction and adhesion-dependent cell survival. Embo J **1998**; 17:6622–32.
36. de Fougerolles AR, Chi-Rosso G, Bajardi A, Gotwals P, Green CD, Koteliansky VE. Global expression analysis of extracellular matrix-integrin interactions in monocytes. Immunity **2000**; 13:749–58.
37. Kim MJ, Wainwright HC, Locketz M, et al. Caseation of human tuberculosis granulomas correlates with elevated host lipid metabolism. EMBO Mol Med **2010**; 2:258–74.
38. Mehra S, Pahar B, Dutta NK, et al. Transcriptional reprogramming in nonhuman primate (rhesus macaque) tuberculosis granulomas. PLoS One **2010**; 5:e12266.
39. Eum SY, Kong JH, Hong MS, et al. Neutrophils are the predominant infected phagocytic cells in the airways of patients with active pulmonary TB. Chest **2010**; 137:122–8.
40. Elkington PT, Emerson JE, Lopez-Pascua LD, et al. *Mycobacterium tuberculosis* up-regulates matrix metalloproteinase-1 secretion from human airway epithelial cells via a p38 MAPK switch. J Immunol **2005**; 175:5333–40.
41. Bifani P, Moghazeh S, Shopsin B, Driscoll J, Ravikovitch A, Kreiswirth BN. Molecular characterization of *Mycobacterium tuberculosis* H37Rv/Ra variants: distinguishing the mycobacterial laboratory strain. J Clin Microbiol **2000**; 38:3200–4.
42. Via LE, Lin PL, Ray SM, et al. Tuberculous granulomas are hypoxic in guinea pigs, rabbits, and nonhuman primates. Infect Immun **2008**; 76:2333–40.
43. Dastur DK, Dave UP. Ultrastructural basis of the vasculopathy in and around brain tuberculomas. Possible significance of altered basement membrane. Am J Pathol **1977**; 89:35–50.
44. Lee YA, Choi HM, Lee SH, et al. Hypoxia differentially affects IL-1beta-stimulated MMP-1 and MMP-13 expression of fibroblast-like synoviocytes in an HIF-1alpha-dependent manner. Rheumatology (Oxford) **2012**; 51:443–50.
45. Volkman HE, Pozos TC, Zheng J, Davis JM, Rawls JF, Ramakrishnan L. Tuberculous granuloma induction via interaction of a bacterial secreted protein with host epithelium. Science **2010**; 327:466–9.
46. Thuong NT, Dunstan SJ, Chau TT, et al. Identification of tuberculosis susceptibility genes with human macrophage gene expression profiles. PLoS Pathog **2008**; 4:e1000229.
47. De Groote MA, Nahid P, Jarlsberg L, et al. Elucidating novel serum biomarkers associated with pulmonary tuberculosis treatment. PLoS One **2013**; 8:e61002.
48. Sellors TH. The results of thoracoplasty in pulmonary tuberculosis. Thorax **1947**; 2:216–23.
49. Jamieson AM, Pasman L, Yu S, et al. Role of tissue protection in lethal respiratory viral-bacterial coinfection. Science **2013**; 340:1230–4.
50. Mayer-Barber KD, Andrade BB, Oland SD, et al. Host-directed therapy of tuberculosis based on interleukin-1 and type I interferon crosstalk. Nature **2014**; 511:99–103.